Verifying the band gap narrowing in tensile strained Ge nanowires by electrical means

OPEN ACCESS
IOP Publishing
Nanotechnology

Nanotechnology **32** (2021) 145711 (5pp)
https://doi.org/10.1088/1361-6528/abd0b2

Verifying the band gap narrowing in tensile strained Ge nanowires by electrical means

M G Bartmann[1,4], M Sistani[1,4], S Glassner[1], B Salem[2], T Baron[2], P Gentile[3], J Smoliner[1] and A Lugstein[1]

[1] Institute of Solid State Electronics, Technische Universität Wien, Gußhausstraße 25-25a, A-1040 Vienna, Austria
[2] Univ. Grenoble Alpes, CNRS, CEA/Leti Minatec, Grenoble INP, LTM, F-38054 Grenoble, France
[3] Univ. Grenoble Alpes, CEA, IRIG- PHELIQS, F-38054 Grenoble, France

E-mail: alois.lugstein@tuwien.ac.at

Received 28 September 2020, revised 13 November 2020
Accepted for publication 4 December 2020
Published 13 January 2021

Abstract

Group-IV based light sources are one of the missing links towards fully CMOS compatible photonic circuits. Combining both silicon process compatibility and a pseudo-direct band gap, germanium is one of the most viable candidates. To overcome the limitation of the indirect band gap and turning germanium in an efficient light emitting material, the application of strain has been proven as a promising approach. So far the experimental verification of strain induced bandgap modifications were based on optical measurements and restricted to moderate strain levels. In this work, we demonstrate a methodology enabling to apply tunable tensile strain to intrinsic germanium $\langle 111 \rangle$ nanowires and simultaneously perform *in situ* optical as well as electrical characterization. Combining I/V measurements and μ-Raman spectroscopy at various strain levels, we determined a decrease of the resistivity by almost three orders of magnitude for strain levels of ~5%. Thereof, we calculated the strain induced band gap narrowing in remarkable accordance to recently published simulation results for moderate strain levels up to 3.6%. Deviations for ultrahigh strain values are discussed with respect to surface reconfiguration and reduced charge carrier scattering time.

Supplementary material for this article is available online

Keywords: germanium, nanowire, strain, band gap narrowing

(Some figures may appear in colour only in the online journal)

The convergence of photonics into a CMOS compatible platform remains a key challenge for the development of future microelectronics technology. Improved functionality and performance such as low-latency and high-bandwidth communication are among the promising outcomes driving this technology. Although great efforts have been invested, a key bottleneck for on-chip photonics is a CMOS-compatible light source [1]. While effective light emitters are natively based on III–V compound semiconductors, the integration of these materials into mature silicon (Si) platform technology requires costly and elaborate heterogenic processing techniques [2]. In contrast, germanium (Ge) can be monolithically integrated in the Si process flow [3, 4] and exhibits a pseudo-direct band gap with a difference in energy of only 136 meV between the direct gap at the Γ-valley (E_g^{Γ} 0.80 eV) and the fundamental indirect gap close to the L-valley (E_g^{L} 0.66 eV) [5]. To overcome the indirect behavior of Ge and thus inefficient photon emission, several approaches have been explored such as modifying the band structure by quantum confinement [6], alloying [7], or strain engineering. Regarding the latter approach, the predicted transformation of Ge to a

[4] These authors have contributed equally to the work.

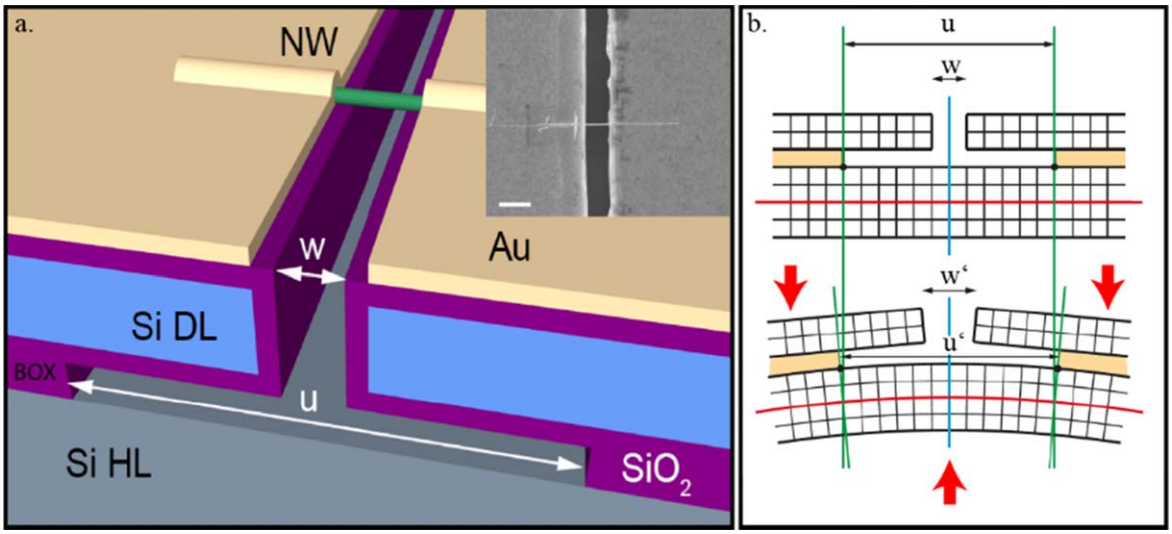

Figure 1. (a) Schematic view of the MSD enabling uniaxial tensile straining of an individual nanowire. The inset shows a close up SEM image of a Ge NW integrated in the MSD. Length and diameter of the utilitzed NWs were ~10 μm and ~120 nm respectively. Scale bar is 1 μm. (b) Shematic cross-section of the MSD in an unbent (top) and bent (bottom) state. The red arrows indicate the applied force via the 3-point bending module.

direct semiconductor [8, 9] at an uniaxial strain of about 5.3% along the ⟨111⟩ direction or biaxial strain of 2.0% triggered a lot of theoretical [8–12] and experimental [5, 13–20] works. Among the manifold techniques, applying uniaxial strain to a quasi-1D Ge nanowires (NW) presents itself as an approach of high potential. In this context, vapor–liquid–solid (VLS) [21] grown Ge NWs were shown to exceed the mechanical strength of their bulk counterpart [22]. This makes them a perfect candidate for strain induced band gap tuning enabling the predicted high strain levels for indirect-direct transition of ≈5.3% [8, 9] and ≈5.7% [8], along the ⟨111⟩ and ⟨001⟩ growth directions, respectively. In this context, experimental works on the measurement of strain induced band gap modifications in Ge were restricted to optical techniques [5, 13, 15, 23] or electrical measurements up to ≈3.5% [14].

In this work, we present an approach enabling to investigate the electrical behavior for VLS grown along the ⟨111⟩ growth direction of Ge NWs for tensile strain up to 5.1%. The uniaxial strain is applied to individual Ge NWs integrated in a micromechanical straining device (MSD) as displayed in figure 1(a). The MSD is based on a silicon on insulator wafer with a handle wafer and device layer thickness of 500 μm and 3 μm respectively. In a first step, trenches about $w = 1.5$ μm wide were patterned in the device layer using optical lithography and reactive ion etching. Subsequently, the underlying 1 μm thick buried oxide was selectively etched using hydrofluoric acid resulting in freestanding Si beams with an underetch of about $u = 120$ μm. To ensure electrical isolation of the MSD, wet thermal oxidation was carried out forming a SiO_2 passivation layer with a thickness of 300 nm resulting in a final trench width of $w = 1$ μm. To complete the device, about 120 nm thick Ge NWs are deposited across the trenches by drop casting. Subsequently, the NWs are fixed by sputter deposited Ti/Au metallic contact pads with a thickness of 200 nm. Figure 1(a) shows the schematic view and the SEM image in the inset of a fully featured MSD with the integrated Ge NW. For the actual investigations, NWs aligned 90° with respect to the trenches were selected to guaranty uniaxial straining and to minimize shear forces in the NW. Finally, the MSD was inserted in a 3-point bending device below a multifunctional confocal μ-Raman setup. Figure 1(b) shows the basic working principle of the MSD: deformation of the MSD as indicated by a 3-point bending (red arrows) exerts tensile strain above the neutral axis (red line) and compressive strain beneath, thus increasing the width of the gap (w'). By controlling the applied force and therefore the degree of bending, the MSD allows for continuous strain tuning of an integrated NW. Based on vector analysis (see supplementary material (available online at stacks.iop.org/NANO/32/145711/mmedia)) the gap width increases with increasing underetch and thus allows the application of amplified strain values compared to a common planar three point bending device.

In-situ strain monitoring was performed by confocal μ-Raman spectroscopy using a green laser ($\lambda = 532$ nm) which was focused on the suspended NW. The application of uniaxial strain along the ⟨111⟩ direction of the Ge NWs causes a redshift of the Ge LO phonon mode [24, 25] which is given by:

$$\Delta\Omega \cong -k * \varepsilon_{\parallel} \quad (1)$$

with $\Delta\Omega$ representing the measured redshift of the Raman LO peak with respect to the unstrained NW, k a crystal orientation dependent material constant [13, 25] and $\varepsilon_{\parallel}$ the strain applied along the Ge ⟨111⟩ NW growth axis. The proportional constant k for uniaxial strain along the ⟨111⟩ direction in Ge NWs was determined by Greil *et al* [13] with $k = 4.34$ cm^{-1}. At this point we want to note, that a strain dependent nonlinearities in Raman shift have been found for strain levels >3% [25]. However, according to the mechanical response of our MSD, we observed no significant nonlinear Raman strain behavior within the investigated strain regime.

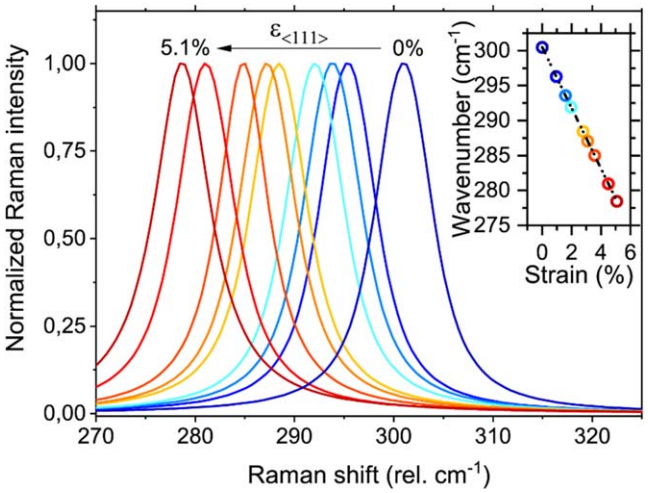

Figure 2. LO-Raman peak of VLS grown ⟨111⟩ Ge NW subjected to increasing uniaxial tensile strain. For the unstrained NW, the raman shift is in accordance with bulk Ge with the main LO peak position at 300.5 rel. cm^{-1}. The inset shows the LO raman peak position as a function of the corresponding strain values.

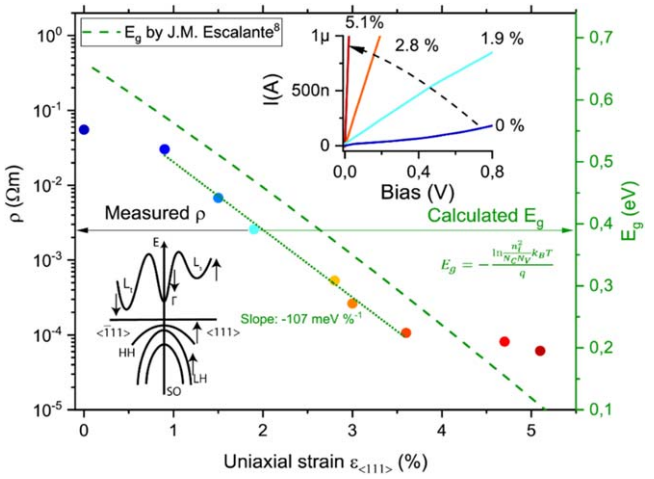

Figure 3. Electrical characteristic of a Ge NW under various uniaxial strain levels shown in figure 2. The resistivity (left *y*-axis,black) was extracted from I/V measurements shown in the top inset. The fundamental band gap E_g extracted from the resistivity by equation (2) is displayed on the right (green axis). The slope of the band gap narrowing with -107 meV %$^{-1}$ is represented by the dotted line. The dashed curve represents the fundamental band gap at the *L*-point under uniaxial strain along the ⟨111⟩ growth direction as recently simulated by J M Escalante [8]. The bottom inset illustrates schematically the bandgap narrowing of tensile strained ⟨111⟩ Ge.

Figure 2 shows the Raman peak shifts for a VLS grown Ge ⟨111⟩ NW integrated in the MSD for various strain levels. The LO Raman peak at 300.5 cm^{-1} for the unstrained about 120 nm thick Ge NW matches well with reported value for bulk Ge [24]. The maximum peak shift of $\Delta\Omega = 22.5$ cm^{-1} before rupture of the NW occurs, corresponds to an applied strain of 5.1%. Immediately after the strain determination, electrical characterization was performed by measuring the I/V characteristics of the suspended NW for various strain levels (top inset in figure 3). The thereof extracted resistivity of the Ge NWs for various strain levels is displayed in the main plot of figure 3. The resistivity of the intrinsic, unstrained NW of $\rho = 5.5 \times 10^{-2}$ Ωm is in good accordance with previously reported values for VLS grown Ge NWs of comparable diameter [26, 27]. However we have to note that this is roughly a factor 8 lower than the resistivity of bulk Ge [28]. Ge NWs in general show a reduced charge carrier mobility as a result of enhanced surface scattering compared to bulk Ge [29]. However, the higher charge carrier density due to surface doping effects [30–34], result in an overall reduced resistivity of Ge NWs with respect to the bulk counterpart.

Starting from the unstrained Ge NW, the resistivity decreases slightly for strain values up to 0.9%. Further straining leads to an exponential decrease until 3.6%. The overall decrease in resistivity by about three orders of magnitude is assumed to be a result of the strain induced modification of the charge carrier density and/or mobility, both closely related to the band structure [28]. It is well known that uniaxial strain will not only modify the band gap energy [14], but also band warping and energy level splitting or shifting [35, 36]. The fundamental band gap (E_g) of Ge at the *L* point in the Brillouinzone, is defined as the distance between the four fold degenerated ($L_{\langle 111\rangle}$, $L_{\langle \bar{1}11\rangle}$, $L_{\langle 1\bar{1}1\rangle}$, $L_{\langle 11\bar{1}\rangle}$) conduction band valleys and the maximum of the also degenerated maximum of the heavy hole (HH) and light hole (LH) valence bands. For uniaxial tensile strain applied along the ⟨111⟩ growth direction of the Ge NW, the $L_{\langle 111\rangle}$ valley is uplifted while the remaining valleys experience a lowering in energy, resulting in a triplet and singlet state with different energies [9]. Thus, the splitting of the degenerated valence band and the uplifting of the HH band in combination with the lowered *L* valley leads to an effective decrease of the band gap energy (see schematic band structure in figure 3). Since the number of charge carriers of an undoped semiconductor with a rather small band gap such as Ge is exponentially dependent on E_g [14], the lowered bandgap will result in an increase of the charge carrier density. Consequently, the resistivity of a strained Ge NW decreases.

In accordance with previous experimental [14] and theoretical [37] work, the mobility of Ge NWs is considered to remain unaffected for low and moderate strain levels. Consequently, one can estimate the band gap in this region via [28]:

$$E_g = -\frac{\ln\left(\frac{n_i^2}{N_C N_V}\right) k_B T}{q} \tag{2}$$

with the carrier concentration n_i extracted from the resistivity values according to

$$n_i = \frac{1}{\rho q(\mu_n + \mu_p)} \tag{3}$$

with ρ the resistivity, k_B the Boltzmann constant, T the temperature, and q the elementary charge. The effective densities of states N_C and N_V in the conduction and valence band, respectively as well as the mobility of electrons (μ_n)

and holes (μ_p) were assumed to be the same as for bulk Ge [14].

The band gap E_g as a function of the applied strain is displayed on the right green y-axis in figure 3, together with the recently simulated data from J M Escalante [8]. Strikingly the experimental data are systematically downshifted. The reason therefore is the above mentioned lower resistivity of intrinsic NWs compared to their bulk counterparts, due to accumulation of charge carriers induced by surface traps [34]. However for strain levels from 0.9% to 3.6% the calculated band gap narrowing of ≈ -107 meV $\%^{-1}$ extracted by a linear fit, is in perfect agreement with JM Escalante.[8] For even higher strain values >3.6% in contradiction to the simulation we observed a flattening of the band gap narrowing with increasing strain. We assume that for such high strain, a modification of the mobility has to be taken into account. The mobility for charge carriers in semiconductors is defined as [28]

$$\mu = \frac{q\tau}{m^*} \tag{4}$$

with τ the scattering time of charge carriers and m^* the respective effective mass. Murphy-Armando *et al* [37] reported, that an uniaxial strain of 4.7% along $\langle 111 \rangle$ in Ge nanowires will lead to an overall electron mobility enhancement by a factor of 5, further increasing with strain. This is mainly governed by an effective electron population of the Γ valley as the distance between L and Γ valley decreases [37]. However, a higher mobility results in a reduced resistivity, which is in the opposite of the experimentally observed behavior.

A possible explanation for this counterintutitive behavior is related to the fact that the application of high strain to NWs result in a reconfiguration of surface states, due to the stress induced modulation of the surface potential [38–40]. This will further result in a redistribution of trap states. According to Winkler *et al* [38], this can overcompensate the mobility improvement due to strain.

Further, it is well known that the scattering time of charge carriers in NWs can be altered by the application of strain [37, 41]. This includes phonon [37, 41, 42], coulomb [41, 43] as well as surface roughness scattering [41, 42, 44]. Consequently, an increased scattering time could additionally counteract the mobility increase by an intervalley scattering induced effective mass reduction.

Conclusions

In conclusion, we demonstrated an MSD enabling the application of uniaxial tensile strain to quasi-1D nanostructures and simultaneous optical and electrical characterization. For VLS grown $\langle 111 \rangle$ oriented Ge NWs we extracted a resistivity change of almost three orders of magnitude for the maximum achievable strain of 5.1% before rupture. In excellent agreement with a very recent theoretical study, we calculated a narrowing of the electronic band gap at the L-point of ≈ -107 meV$\%^{-1}$ from a resistivity dependent model. For strain values above 3.5%, increased strain induced surface reconfiguration and altered scattering time of charge carriers appear to be the most reasonable candidates for the observed strong deviation from the applied model. As this approach is not limited to Ge it may in general contribute to a better understanding of highly strained nanostructures complementary to optical investigations.

Acknowledgments

The authors gratefully acknowledge financial support by the Austrian Science Fund (FWF): Project No. P29729-N27 and P28175-N27. The authors further thank the Center for Micro- and Nanostructures for providing the cleanroom facilities.

Author's contributions

M G B and M S contributed equally to this work. M G B wrote the manuscript, M G B, M S and S G performed the fabrication of the samples and conducted the electrical and optical measurements. B S, T B and P G synthesized the Ge NWs. J S provided expertize on experimental and theoretical interpretations. A L conceived the project and contributed essentially to the experimental design.

ORCID iDs

M G Bartmann https://orcid.org/0000-0002-9556-1550
M Sistani https://orcid.org/0000-0001-5730-234X
B Salem https://orcid.org/0000-0001-8038-3205
A Lugstein https://orcid.org/0000-0001-5693-4775

References

[1] Zhou Z, Yin B and Michel J 2015 On-chip light sources for silicon photonics *Light: Sci. Appl.* **4** e358–358
[2] Ramirez J M *et al* 2020 III-V-on-silicon integration: from hybrid devices to heterogeneous photonic integrated circuits *IEEE J. Sel. Top. Quantum Electron.* **26** 1–13
[3] Tsuchizawa T, Yamada K, Watanabe T, Park S, Nishi H, Kou R, Shinojima H and Itabashi S I 2011 Monolithic integration of silicon-, germanium-, and silica-based optical devices for telecommunications applications *IEEE J. Sel. Top. Quantum Electron.* **17** 516–25
[4] Chen C, Li C, Huang S, Zheng Y, Lai H and Chen S 2012 Epitaxial growth of germanium on silicon for light emitters *Int. J. Photoenergy* **2012** 1–8
[5] Guilloy K *et al* 2016 Germanium under high tensile stress: nonlinear dependence of direct band gap versus strain *ACS Photonics* **3** 1907–11
[6] Cosentino S *et al* 2015 The role of the interface in germanium quantum dots: when not only size matters for quantum confinement effects *Nanoscale* **7** 11401–8
[7] Wirths S *et al* 2015 Lasing in direct-bandgap GeSn alloy grown on Si *Nat. Photon.* **9** 88–92

[8] Escalante J M 2018 Non-linear behavior of germanium electronic band structure under high strain *Comput. Mater. Sci.* **152** 223–7

[9] Zhang F, Crespi V H and Zhang P 2009 Prediction that uniaxial tension along ⟨111⟩ produces a direct band gap in germanium *Phys. Rev. Lett.* **102** 156401

[10] Lee M L, Fitzgerald E A, Bulsara M T, Currie M T and Lochtefeld A 2005 Strained Si, SiGe, and Ge channels for high-mobility metal-oxide-semiconductor field-effect transistors *J. Appl. Phys.* **97** 011101

[11] Tahini H, Chroneos A, Grimes R W, Schwingenschlögl U and Dimoulas A 2012 Strain-induced changes to the electronic structure of germanium *J. Phys.: Condens. Matter* **24** 195802

[12] Liu J, Sun X, Pan D, Wang X, Kimerling L C, Koch T L and Michel J 2007 Tensile-strained, n-type Ge as a gain medium for monolithic laser integration on Si *Opt. Express* **15** 11272

[13] Greil J, Lugstein A, Zeiner C, Strasser G and Bertagnolli E 2012 Tuning the electro-optical properties of germanium nanowires by tensile strain *Nano Lett.* **12** 6230–4

[14] Ran S, Glen T S, Li B, Shi D, Choi I-S, Fitzgerald E A and Boles S T 2020 The limits of electromechanical coupling in highly-tensile strained germanium *Nano Lett.* **20** 3492–8

[15] Guilloy K, Pauc N, Gassenq A, Gentile P, Tardif S, Rieutord F and Calvo V 2015 Tensile strained germanium nanowires measured by photocurrent spectroscopy and x-ray microdiffraction *Nano Lett.* **15** 2429–33

[16] Al-Attili A Z, Kako S, Husain M K, Gardes F Y, Iwamoto S, Arakawa Y and Saito S 2016 Tensile strain engineering of germanium micro-disks on free-standing SiO_2 beams *Japan. J. Appl. Phys.* **55** 04EH02

[17] Ayan A, Turkay D, Unlu B, Naghinazhadahmadi P, Oliaei S N B, Boztug C and Yerci S 2019 Strain engineering of germanium nanobeams by electrostatic actuation *Sci. Rep.* **9** 4963

[18] Huo Y, Lin H, Chen R, Makarova M, Rong Y, Li M, Kamins T I, Vuckovic J and Harris J S 2011 Strong enhancement of direct transition photoluminescence with highly tensile-strained Ge grown by molecular beam epitaxy *Appl. Phys. Lett.* **98** 011111

[19] Ghrib A, El Kurdi M, de Kersauson M, Prost M, Sauvage S, Checoury X, Beaudoin G, Sagnes I and Boucaud P 2013 Tensile-strained germanium microdisks *Appl. Phys. Lett.* **102** 221112

[20] Sanchez-Perez J R, Boztug C, Chen F, Sudradjat F F, Paskiewicz D M, Jacobson R, Lagally M G and Paiella R 2011 Direct-bandgap light-emitting germanium in tensilely strained nanomembranes *Proc. Natl Acad. Sci.* **108** 18893–8

[21] Ray S K, Katiyar A K and Raychaudhuri A K 2017 One-dimensional Si/Ge nanowires and their heterostructures for multifunctional applications—a review *Nanotechnology* **28** 092001

[22] Ngo L T, Almécija D, Sader J E, Daly B, Petkov N, Holmes J D, Erts D and Boland J J 2006 Ultimate-strength germanium nanowires *Nano Lett.* **6** 2964–8

[23] Jiang J *et al* 2019 Strain-induced enhancement of electroluminescence from highly strained germanium light-emitting diodes *ACS Photonics* **6** 915–23

[24] Cerdeira F, Buchenauer C J, Pollak F H and Cardona M 1972 Stress-induced shifts of first-order raman frequencies of diamond- and zinc-blende-type semiconductors *Phys. Rev.* B **5** 580–93

[25] Gassenq A *et al* 2017 Raman-strain relations in highly strained Ge: uniaxial ⟨100⟩, ⟨110⟩ and biaxial (001) stress *J. Appl. Phys.* **121** 055702

[26] Seifner M S, Sistani M, Porrati F, Di Prima G, Pertl P, Huth M, Lugstein A and Barth S 2018 Direct synthesis of hyperdoped germanium nanowires *ACS Nano* **12** 1236–41

[27] Koleśnik-Gray M M, Lutz T, Collins G, Biswas S, Holmes J D and Krstić V 2013 Contact resistivity and suppression of Fermi level pinning in side-contacted germanium nanowires *Appl. Phys. Lett.* **103** 153101

[28] Sze S M and Ng K K 2006 *Physics of Semiconductor Devices* 3 (Hoboken, NJ, USA: John Wiley & Sons, Inc.) (https://doi.org/10.1002/0470068329)

[29] Tanaka H, Suda J and Kimoto T 2015 Impacts of surface roughness scattering on hole mobility in germanium nanowires *2015 Silicon Nanoelectron. Work. SNW* vol 2015, pp 1–2

[30] Sistani M, Staudinger P, Greil J, Holzbauer M, Detz H, Bertagnolli E and Lugstein A 2017 Room-temperature quantum ballistic transport in monolithic ultrascaled Al–Ge–Al nanowire heterostructures *Nano Lett.* **17** 4556–61

[31] Hanrath T and Korgel B A 2005 Influence of surface states on electron transport through intrinsic Ge nanowires *J. Phys. Chem.* B **109** 5518–24

[32] Zhang S, Hemesath E R, Perea D E, Wijaya E, Lensch-Falk J L and Lauhon L J 2009 Relative influence of surface states and bulk impurities on the electrical properties of Ge nanowires *Nano Lett.* **9** 3268–74

[33] Tsipas P and Dimoulas A 2009 Modeling of negatively charged states at the Ge surface and interfaces *Appl. Phys. Lett.* **94** 012114

[34] Sistani M, Staudinger P and Lugstein A 2020 Polarity control in ge nanowires by electronic surface doping *J. Phys. Chem.* C **124** 19858–63

[35] Sun Y, Thompson S E and Nishida T 2010 *Strain Effect in Semiconductors* (Boston, MA: Springer US) (https://doi.org/10.1007/978-1-4419-0552-9)

[36] Fischetti M V and Laux S E 1996 Band structure, deformation potentials, and carrier mobility in strained Si Ge, and SiGe alloys *J. Appl. Phys.* **80** 2234–52

[37] Murphy-Armando F and Fahy S 2011 Giant enhancement of n-type carrier mobility in highly strained germanium nanostructures *J. Appl. Phys.* **109** 113703

[38] Winkler K, Bertagnolli E and Lugstein A 2015 Origin of anomalous piezoresistive effects in VLS grown Si nanowires *Nano Lett.* **15** 1780–5

[39] Rowe A C H 2008 Silicon nanowires feel the pinch *Nat. Nanotechnol.* **3** 311–2

[40] Milne J S, Rowe A C H, Arscott S and Renner C 2010 Giant piezoresistance effects in silicon nanowires and microwires *Phys. Rev. Lett.* **105** 226802

[41] Baykan M O, Thompson S E and Nishida T 2010 Strain effects on three-dimensional, two-dimensional, and one-dimensional silicon logic devices: predicting the future of strained silicon *J. Appl. Phys.* **108** 093716

[42] Fischetti M V, Ren Z, Solomon P M, Yang M and Rim K 2003 Six-band k · p calculation of the hole mobility in silicon inversion layers: dependence on surface orientation, strain, and silicon thickness *J. Appl. Phys.* **94** 1079–95

[43] Weber O and Takagi S 2008 Experimental examination and physical understanding of the coulomb scattering mobility in strained-Si nMOSFETs *IEEE Trans. Electron Devices* **55** 2386–96

[44] Jin S, Fischetti M V and Tang T 2007 Modeling of electron mobility in gated silicon nanowires at room temperature: surface roughness scattering, dielectric screening, and band nonparabolicity *J. Appl. Phys.* **102** 083715